

Testing and performance evaluation of terrestrial panoramic imaging system in close range documentations

Anastasios – Grammatas Kampouris, Evangelia Lambrou

Abstract—A new surveying methodology is accomplished by using terrestrial integrated panoramic imaging systems from fixed station. This technique promises to reduce the surveyor's field work time in some minutes in order to facilitate the visual and geometrical documentation of various objects and enrich the deliverables of the survey. This paper investigates the convenience of the methodology pushing forward the advantages and the disadvantages. Additionally, compares the results of two selected applications which were respectively implemented by conventional terrestrial survey. The experimental applications that were carried out involved in surveying and documenting a building façade and a vertical cylindrical fuel storage tank. The comparison deals with the accuracy achieved and the time needed for the field work as well as for the data processing. The instrumentation used was the Trimble V10 imaging rover and first order total stations. Thus panoramic imagery from fixed stations is proved to be applicable for the most common survey applications as well as building facades and geometric documentation of structures. The provided accuracy of the calculated coordinates is of the order of few centimeters.

Index Terms—V10 imaging rover, façade, monument documentation, accuracy, panorama imagery.

I. INTRODUCTION

Surveying by using a total station is considered to be the primary technique and methodology. So today with the rapid development of the total station's technology, this kind of instrumentation has become "smart" when it's integrated with GNSS [1], robotic [2], servomotorised, imaging [3] offering a multitude of applications that facilitate, accelerate and develop the field work. Contemporary total stations can also execute reflectorless distance measurements and perform light-scanning so as to create meshes and 3D models [4]. On the other hand, single terrestrial metric cameras are being used since nowadays in various applications. An initial step was the construction of stereocameras which provided a known arrangement of them. The issues occurred by their use, had to do with the limitation of the ratio between the baseline and the object distance which is vital in such operations. The solution was provided by the establishment of photo-theodolites that could be placed on known positions and the camera's orientation could be measured on the field [5]. Additionally, the most advanced camera survey instruments are referred to spherical or panoramic imaging systems for the needs of vehicle-based photogrammetry (mobile mapping). These systems are intended to produce photo-realistic three-dimensional cartographic illustrations.

On the vehicle there are also installed tilt sensors (IMU: Inertial Measurement Units) as long as with GNSS receivers (mostly GPS) to record the platform's orientation and position respectively along time [6].

Finally the evolution of terrestrial photogrammetric and geodetic instrumentation has led to the creation of integrated panoramic camera systems. These multicamera systems have the ability to combine geodetic and photogrammetric techniques for the confrontation and conduction of the survey. As a result the estimated time of the whole survey can be reduced and lead to rapid construction of 3D models and texture mapping deliverables [7].

In this paper a brief presentation of the planning process of a close range photogrammetric project is attempted by using a panoramic imaging system. Also two characteristic experimental applications were carried out in order to assess the whole procedure about the convenience, the time needed, the provided accuracy and the quality of the results. The evaluation became by comparing the panoramic imaging system derivatives to the corresponding ones, which have derived by using first order total station and conventional surveying techniques.

II. IMPLEMENTING A TERRESTRIAL SURVEY PROJECT WITH A PANORAMIC IMAGING SYSTEM

A. Planning Parameters (From Conception to Confrontation)

The development of a close-range photogrammetric project includes many design aspects like the mean image scale, the photogrammetric algorithms, the measuring accuracy of image coordinates, the position of the images, the camera's characteristics (image format, focal length), the calibration parameters, the optical parameters etc.

In most cases an integrated panoramic imaging system exempts the practitioner from this typical workflow. This happens because it consists of several hard mounted cameras, where their optical parameters are fixed and the knowledge of their interior orientation parameters as well as their relative orientation is carried out at an earlier stage and is considered known [8].

The quality and the accuracy of the final geometric derivatives begin with the choice of the mean image scale $\frac{1}{\kappa} = \frac{c}{d}$, which is degenerated into the distance (d) between the object and the panorama as the constant (c) of the cameras

is constraint. Certainly it is impossible to maintain the mean scale among the images of a panorama, but only as regards a particular object or a specific area.

As it is well known, a photo camera can be considered as an instrument which is recording directions. Thus, the primary operating principle of an imaging system is the photogrammetric intersection, which is simply accomplished by the intersection of at least two homologous beelines in the 3D space [5]. Firstly the pixel size with respect to the constant (c) of the camera and the measuring accuracy in the image, form a particular angular uncertainty which corresponds to a spatial resolution that is linearly scaled through the object distance (d).

Moreover the uncertainty of the photogrammetric intersection corresponds to the limitation of the ratio between the object distance (d) and the base length (b) of two panoramas, so that the intersecting angle to be neither particularly acute nor obtuse. The optimal case is when the intersecting angle is right (100grad), hence the baseline (b) of two panoramas is twice the object distance (d) $b=2d$.

However the ratio among the object distance and the baseline is not enough if the goal is the homogeneity along 3D accuracy. This means that the predetermined parameters of a panoramic imaging system create boundaries on dimensioning these two distances. This can easily be accomplished and calculated by using the error propagation law and the relations of a set of true vertical pictures.

Thus, according to the aforementioned criteria the user can choose the optimum positions to capture the panoramas and proceed to the confrontation of the survey by using an integrated panoramic imaging system.

B. Survey implementation

The imaging system can be used as a typical camera of a photogrammetric project with the use of photo observable control points on the object. Otherwise the control points can be reduced or eliminated by the use of the photo station's coordinates and measurements of the internal sensors of the camera head. The station's coordinates and the raw values of the sensors can be utilized either as values of the external orientation of the panorama or as approximate values in accordance to the selected mathematical model of the bundle adjustment process [9]

The implementation of a survey application with an imaging system typically starts with the data acquisition. This initial step, which is considered as the most crucial part of the whole process, includes the configuration of the photo stations' positions; the measurement of the photo stations' coordinates as well as the control points' and the check points' and finally the capturing of the panoramas. The photo stations' geometry with respect to the object of study is a matter of vital importance because it affects the quality and the accuracy of the entire survey.

The second stage of the survey is the data post processing which is performed on appropriate software. This stage

comprises the panoramas bundle adjustment and then the observations of the object's characteristic points.

Subsequently the bundle adjustment of the panoramas is resolved by measuring the necessary amount of corresponding tie points, which have to be normally distributed both horizontally and vertically on the panoramas range. The tie points can be measured either manually or automatically, by using a matching technique. As much better is the geometry of the photogrammetric network and the solution of the bundle adjustment the smaller the error propagation is on the object's characteristics points.

III. COMPARING PROCEDURE AND INSTRUMENTATION

Two experimental applications took place in parallel with conventional methodologies and instrumentation (reflectorless total station, imaging station scanning) so as to contrast the different procedures and compare their geometric derivatives and deliverables.

A building facade and a vertical cylindrical fuel storage tank are surveyed and documented. In both applications the panoramas were captured by placing the imaging system on known survey points, which were initially measured via total station. Moreover the mathematical model selected to resolve the terrestrial triangulation of the panoramas allowed the correction of only three rotations for each with respect to the photo station coordinates. Hence the propagation of errors is minimized and the procedure is exempted from the use of photo-observable control points on the object or the surroundings.

The V10 Imaging Rover is used as well as the VX imaging total station. The nominal angular accuracy of the station is $\pm 1''$ as the distance measuring accuracy with a prism is $\pm 2\text{mm} \pm 2\text{ppm}$ and without a prism is $\pm 5\text{mm}$ ($< 250\text{m}$) and the scanning rate is 15 points per sec [10].

It is also worth to describe the main characteristics of the imaging system V10 Imaging Rover. The integrated camera system V10 Imaging Rover is consisted by three main parts: the head, a positioning sensor and the supporting software. The main body of V10 is comprised of the rod, the bipod, the control unit and the camera head (fig. 1). The positioning sensor is fitted on the top of the camera head and may be either a GNSS receiver, mostly on VRS operation mode, or a 360° prism for the monitoring of the system via a robotic total station on autolock operation mode [11]. The camera system of V10 consists of 12 cameras, the upper row with 7 panorama cameras with landscape orientation and the lower row with 5 down-looking cameras with portrait orientation [12]. The major sensors that are contained in the V10 camera head are two tilt sensors, which measure the system's deviation from verticality along two axes, and a magnetic compass, which measures the panorama's magnetic azimuth.

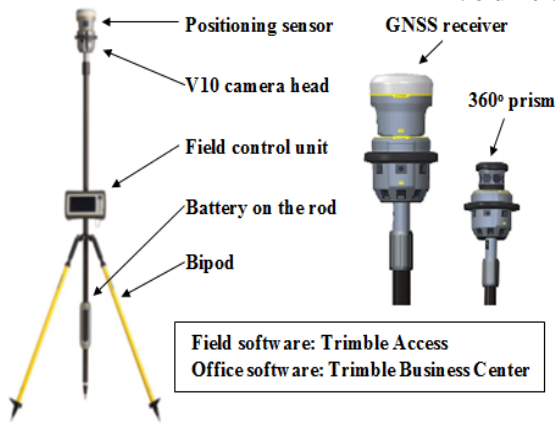


Fig 1: The components of V10 Imaging Rover

IV. SURVEYING A BUILDING FAÇADE

The first application that was attempted involved in surveying a building facade (fig.2), which length was about 30meters. The implementation of the survey by using the V10 imaging rover was carried out twice with different multitude and configuration of the 8 photo stations (fig. 3) and different observation process for the tie points extraction.



Fig 2: Part of the panorama imagery of the façade.

Firstly, the survey conducted by capturing 6 panoramas from the stations S1, S2, S3, S4, S5 and S6, which perform 3 pairs of stations, and executing an automatic tie points extraction. The automatic matching technique observed 620 tie points and the triangulation resolved with 792 degrees of freedom and a-posteriori standard deviation of ±0.7pixels. Finally the geodetic coordinates of 85 points of the facade were calculated via manual photogrammetric observations that were carried out.

The poor geometry of the photo stations and the large residuals of the points observations led to the densification of the photogrammetric network with two more acquired panoramas from the stations S7 and S8 (fig. 3) and a second approach of the survey. The bundle adjustment was then resolved with 20 manually observed tie points, 138 degrees of freedom and a-posteriori standard deviation of ±0.59pixels. Afterwards 86 points of the façade’s plane were manually measured.

The time needed for the completion of the survey by using the imagine system was only 30 minutes for the panoramas capturing. Also about 1.5 hours were needed for the photo stations coordinates determination by using conventional methods. Namely 2 hours for the field work and 6 hours for the data elaboration. Additionally the allocation of the time needed with the conventional method was 6 hours for field

work and 3 hours for the office work. At this point should be highlighted that there is a large overlap between the field work times of the two methods. Therefore the overall time needed for the survey with the imagine system is reduced especially in terms of time of the field work.

The determination of the geometric alteration of the drawings (fig. 4), which have derived from the use of the imagine system with respect to the one of the conventional method, was accomplished by measuring the vector of the difference between the position of corresponding characteristics points (ds), the bearing and its components along x (dx) and y (dy) axes. The mean values of the parameters \overline{ds} , \overline{dx} , \overline{dy} were estimated according to the equation (1).

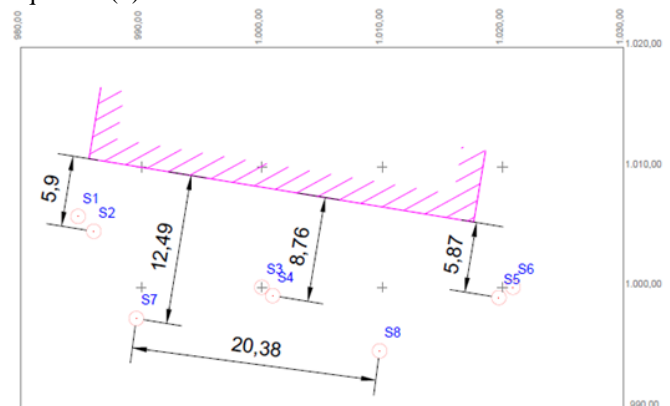


Fig 3 Configuration of photo stations.

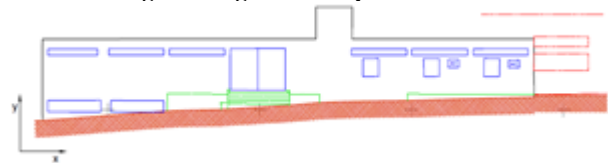


Fig 4 The drawing of the building’s façade.

$$\overline{dx} = \frac{1}{n} \sum_1^n |dx| \tag{1}$$

Table 1 presents the minimum, the maximum and the mean values of ds, dx and dy for both the automatic and the manual bundle adjustment process.

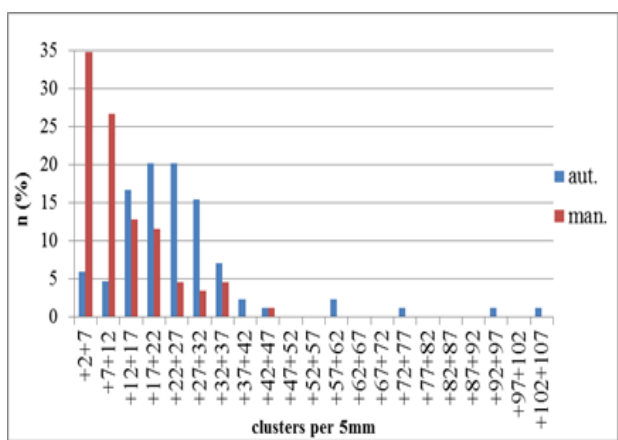
Furthermore the drawings were separated in three vertical sections, the western, the central and the eastern and the mean values of the alteration (ds) were then recalculated. The results are evidencing that the 2D drawings are strengthened in the center because the parameters of the photogrammetric intersections are optimized among this region of the model.

Table 1. The minimum, the maximum and the mean values of ds, dx and dy.

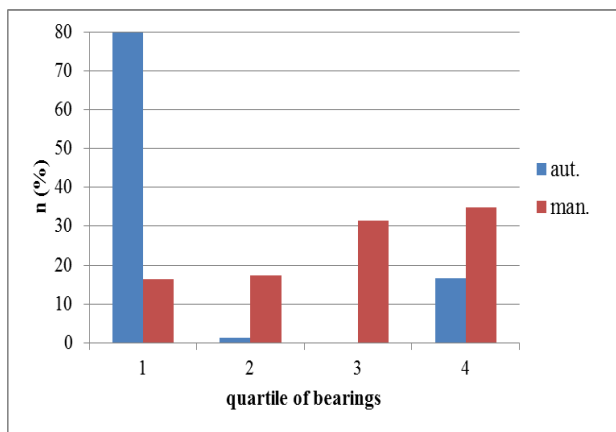
	ds(mm)			Western	Central	Eastern
	min.	Max.	mean	mean ds(mm)		
Automatic	2	103	25	29	19	31
Manual	2	43	13	18	9	13
	dx(mm)			dy(mm)		
	min.	Max.	mean	min.	Max.	mean
Automatic	-89	102	16	-2	39	17
Manual	-33	35	9	-32	21	6

The histogram of figure 5 (a) represents the percentage distribution of point position change vectors by clustering at intervals of 5mm. On the other hand the histogram of the figure 5 (b) shows the percentage distribution of the clockwise bearing of the vectors per quartile, where a systematic error of panoramas orientation is detected when the automatic process was used. Thus the drawing seems to be quite super elevated with respect to the one of the conventional method due to the poor geometry of the network of the photo stations.

On the contrary the densification of the photo stations and the manual bundle adjustment of the panoramas managed to improve the results. Moreover the bearing of the vectors seems to be normally distributed.



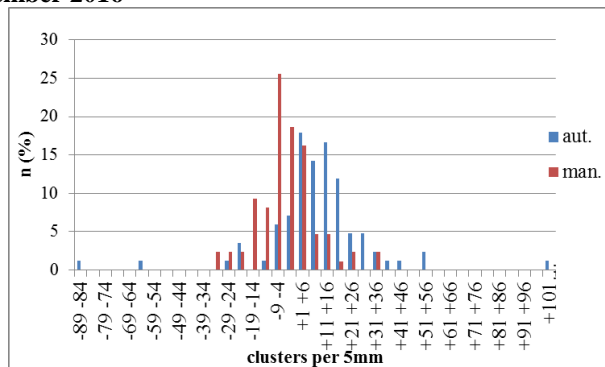
ds (a)



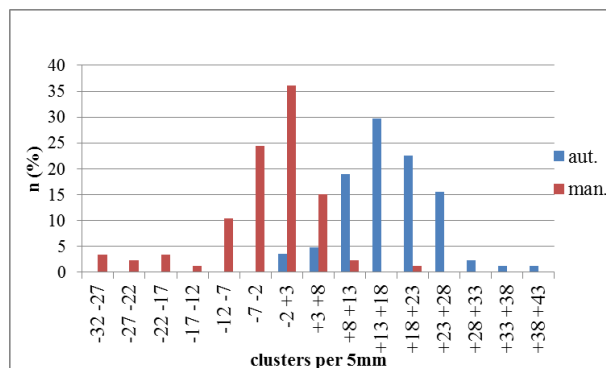
(b)

Fig 5 Distribution of point's position change vectors ds (a) and bearings (b) in respect to the automatic or manual bundle adjustment process.

Thereafter the histograms of figure 6 represents the percentage distribution of \overline{dx} (fig. 6a) and of \overline{dy} (fig. 6b) of the drawings with the same clustering. Even though the mean value of elevations difference (dy) of the automatic process seems to be bigger, the range of the values is demonstrating that they are determined with better accuracy. Hence the elevation alteration is less than the horizontal, as it is expected in close range photogrammetric applications [5].



dx (a)



dy (b)

Fig 6 Distribution of differences dx (a) and dy (b) in respect to the automatic or manual bundle adjustment process.

V. DETECTION OF DEFORMATIONS OF A VERTICAL CYLINDRICAL FUEL STORAGE TANK

The external calibration of a vertical cylindrical fuel storage tank also attempted with the use of a panoramic imaging system. The P-736 tank was selected which is located in the industrial facilities of Aspropyrgos refinery in western Attica Greece (fig. 7). What is needed to be highlighted is that none of the methodologies that were carried out is authorized by international organizations (ISO, API) for tank calibration operations.



Fig 7. The fuel storage tank.

The nominal radius value of the tank is 11.5m and its height is 13.4m. Thus, according to ISO-7507 and API-653 the

radius computations must be under the threshold uncertainty of $\pm 2\text{mm}$ [13] – [14] – [15].

Moreover, the fill level of the tank remained constant during the measurements at about 8m with an additional specific weight of fluid at 0.8kg/lt. Hence, the instant deformation of the tank due to hydrostatic pressure, which has a maximum value of about 3mm with respect to the radius of the lowest ring, was constraint and was not taken under consideration [14].

There were 16 stations (S1-S16) measured on a local system by using the total station (fig. 8). The stations coordinates were calculated with an accuracy of $\pm 3\text{mm}$. The stations S1-S8 were placed on the top edge of the surround declivity; therefore they were elevated about 2.5m higher in relation to the stations S9-S16.

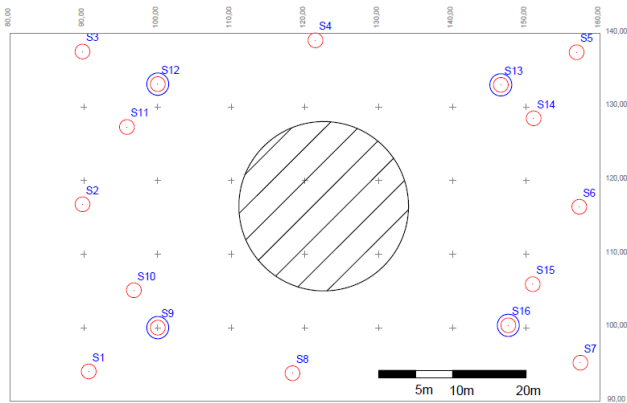


Fig 8. Plan view of the tank and the stations.

The implementation of the tank's calibration by using the imaging system started with the panorama acquiring from each one of the 16 stations.

The bundle adjustment of the panoramas was then conducted through a combination of automatic and manual tie point extraction. Thus, the bundle adjustment of the 16 photo stations resolved with 1214 tie points and 2018 degrees of freedom. The a-posteriori standard deviation of the observations was calculated at $\pm 0.46\text{pixels}$. Then 89 discrete points of the tank's shell were measured manually among six specific horizontal cross sections in different height levels of the construction. The six horizontal cross sections are defined per about two meters interval on the tank's shell (fig. 9).

Thereafter the survey carried out by using the total station, which combines surveying, imaging and scanning. The tank shell was scanned from 4 stations (S9, S12, S13, and S16) (fig. 8) with a scanning step of 20cm (for both horizontal and vertical directions) and a small space of overlapping between the different point clouds.

The removal of the unneeded points and the creation of the mesh (fig. 10) continued via appropriate software. There were 6 horizontal cross sections of the mesh extracted in the same height levels as the ones of the discrete points of the imaging system measurements on its accompanying software. The processed point cloud, which is consisted of 30000 points, was also cut into 6 horizontal planar layers in the same height levels with a thickness of 5cm.



Fig 9. The six horizontal cross sections on the tank's shell.

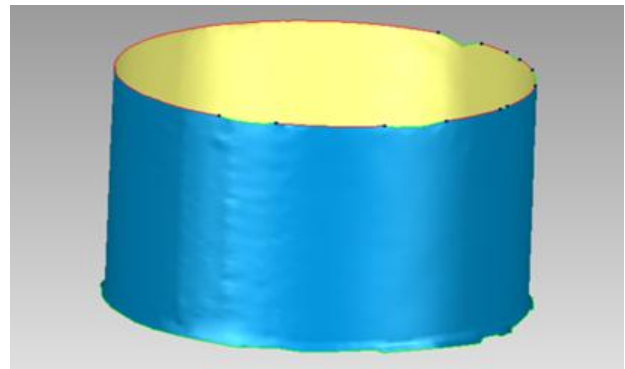


Fig 10 The tank's mesh creation by the total station scanning.

The time that was needed for the survey of the tank by using the imaging system was only about 1 hour for capturing the panoramas and 2 hours for the configuration and the measurements of the photo stations coordinates by using the total station. Totally 3 hours for the field work and 10 hours for the data processing were needed. On the other hand the time needed with the scanning method by using the total station was 5 hours for field work and 5 hours for the data processing.

The comparison between the geometric derivatives of the two methodologies took place in two different ways. Firstly by fitting a circle (eq. 2) to the discrete points of the imaging system and the planar point clouds of the total station at six horizontal sections of the tank's shell. The adjustment carried out with the formation of an algorithm according to the general least squares method [16] – [17]. The unknowns of the process are the coordinates of the center (x_c, y_c) and the radius (R) of the fitted circle.

$$f_i(\bar{x}, \bar{l}) = (x_i - x_c)^2 + (y_i - y_c)^2 - R^2 = 0 \quad (2)$$

Where x_i, y_i : the geodetic coordinates of the measured point i The results along with their standard deviations of the circle fitting procedure for the imaging system and the total station points are represented in the table 2 and 3 respectively. The accuracy of the results is much better than the average precision of the raw points datasets, as it was expected.

Moreover the permanent deformations of the tank's shell due to hydrostatic pressure are detected through the

increasing of the radius opposed to the section's height level for both processes.

	cross section					
	ring1	ring2	ring3	ring4	ring5	ring6
h [m]	11.872	13.730	15.583	17.438	19.288	21.132
points	21	17	17	13	11	10
x _c [m]	122.50 6	122.50 7	122.50 2	122.50 2	122.50 7	122.52 8
σ _{xc} [mm]	±6	±5	±6	±6	±7	±14
y _c [m]	116.48 5	116.48 4	116.48 9	116.48 5	116.48 8	116.48 3
σ _{yc} [mm]	±6	±4	±5	±5	±6	±14
R [m]	11.514	11.512	11.512	11.511	11.501	11.480
σ _R [mm]	±4	±3	±4	±4	±5	±12
σ ₀ [mm]	±20	±17	±15	±13	±14	±21

Table 2. Parameters of the imaging system points adjustment.

	cross section					
	ring1	ring2	ring3	ring4	ring5	ring6
h [m]	11.872	13.730	15.583	17.438	19.288	21.132
points	127	89	108	98	96	114
x _c [m]	122.50 4	122.50 4	122.50 4	122.50 8	122.51 1	122.51 4
σ _{xc} [mm]	±1	±2	±2	±1	±2	±2
y _c [m]	116.47 9	116.47 3	116.48 0	116.47 3	116.48 0	116.48 0
σ _{yc} [mm]	±1	±3	±2	±2	±3	±2
R [m]	11.510	11.512	11.507	11.504	11.500	11.500
σ _R [mm]	±1	±2	±2	±1	±2	±2
σ ₀ [mm]	±10	±15	±13	±10	±15	±13

Table 3. Parameters of the total station points adjustment.

The determination uncertainty of the parameters x, y and R which achieved by the imaging system measurements are double or triple with respect to the ones of the total station. Even though, the radius determination accuracy through the imaging system points is over the required threshold uncertainty for detecting instant deformations of the tank's shell, due to hydrostatic pressure. Thus the imaging system does not fulfill the calibration accuracy requirements [13] which lead to the formation of the tank's capacity table.

The comparison of the circle fitting parameters among the two datasets took place for a 95% confidence level (z_{0.95}=1.96). The hypothesis test conducted in accordance with the inequality of the eq.3 [17]. All the parameters managed to pass the test except the y_c coordinate of ring 4.

$$-z_p \cdot \sigma_{\Delta x_{ij}} \leq \Delta x_{ij} \leq +z_p \cdot \sigma_{\Delta x_{ij}} \quad (3)$$

Where $\Delta x_{ij} = x_j - x_i$ and $\sigma_{\Delta x_{ij}} = \sqrt{\sigma_{x_j}^2 + \sigma_{x_i}^2}$

Thereafter the horizontal differences (ds) of the imaging system points were measured radically with respect to the estimated centers of the adjustments and the cross sections of the mesh which is created by the total station. The points that were enclosed within the section had a negative value of alteration and those that were outside had a positive value.

Figure 11 presents the difference for each point. The mean value of the horizontal difference of the 89 points, which have derived from the use of the imaging system, was estimated according to eq.1 at 14mm with minimum and maximum of -29mm and 37mm respectively.

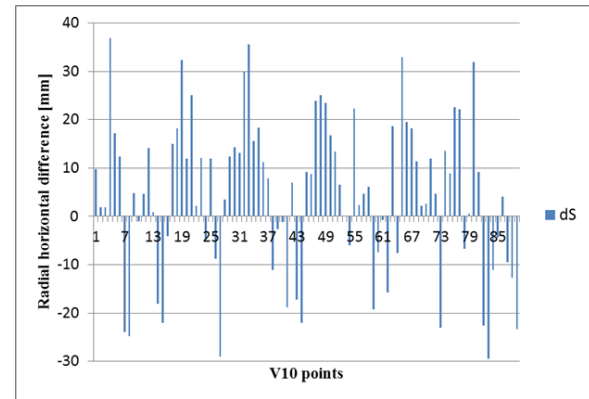


Fig 11 Radial horizontal differences of the imaging system points.

VI. CONCLUSIONS

In this study the potential of a new technique by using an integrated panoramic imaging system is investigated on the implementation of specialized and demanding surveying applications, such as geometrical documentations and deformation measurements. The aforementioned experimental applications suggest the following conclusions.

The use of the multi camera imaging system provides a combination of rapidity, stability and reliability for the geometric derivatives of the survey. The data acquisition is faster than all the other three methodologies and instrumentations, thus the necessary field work time is reduced even to one fifth when the details of the survey are increased.

Every panorama capturing lasts less than five minutes. So the use of a GNSS sensor for the photo stations coordinates determination it will be very convenient and quick if accuracy of some cm is demanded. Otherwise the conventional methods could provide ±2mm, by spending 1-2 hours for the photo stations network's measurement.

On the other hand the data processing time is increased, depending on the user's options and the level of detail in measuring discrete points photogrammetrically.

Panoramic imaging systems are proved to be an easy to use tool, even though that they are totally dependent on a positioning sensor, which affects the overall accuracy of the survey.

Moreover the functionality of these systems largely depends on the environmental conditions (e.g. brightness) and the existence of texture on the surfaces. For instance, the matching technique failed to resolve panoramas that were captured at a different time (without the HDR technique), although the surfaces were neither smooth nor monochrome. Whereas one part of the storage tank could not be exploited

due to the intense sunlight and the white color of the construction.

The poor solution of the bundle adjustment leads to larger differences of the final product of the order of 10cm in respect to the accurate terrestrial survey. These differences are eliminated to 1-2cm when the solution of the bundle adjustment is strengthened. The comparison that took place between different datasets, which all of them containing errors, identifies an approximate estimation for the quality of the geometric derivatives of the imaging system and not the standardized measuring accuracy of the system.

Hence, in an optimized procedure, where there are the appropriate conditions and principles of use (e.g. ratio of base length to object distance, $0.5d \leq b \leq 2.5d$), the object distance is the most crucial parameter that affects the point's coordinates accuracy. Thus the accuracy that can be achieved on measuring point's coordinates, when the object distance is about 10m, is of the order of ± 1 cm. This implies that 2D drawings of horizontal and vertical sections can be constructed as well as 3D models with a maximum print scale of 1:50.

Furthermore the quality of the solution of the bundle adjustment of the panoramas is affected more from the photo station geometry, the distribution of the tie points and their intersection conditions than the degrees of freedom, which is also an established point of view of the manufacturer. The height difference among the photo stations appears to enhance the geometry of the photogrammetric network and facilitates a better distribution of the tie points.

Also, the stability of the geometric data of the imaging system enables the statistical processing of it. So by adjusting measured points on a tank's circumference with nominal radius value of 11.5m, according to the necessary statistical tests, the imaging system was able to measure it with a mean uncertainty of only ± 5 mm. The quality of these measurements is sufficient for the determination of permanent deformations of the tank's shell roundness but not for the calculation of instant deformations due to hydrostatic pressure. Therefore the calibration of the tank (ISO 7507) and the formation of its capacity table cannot be supported.

Consequently, the overall results of the imagine system are very propitious as accuracy of few millimeters was achieved. Further investigation for the use of such systems in more complicated documentations as monuments survey is interesting to be elaborate. Also a thorough research must be carried out in order to optimize the number and the position, where the imagine system should be placed, as this is emerged as the most crucial parameter, which influences the achieved accuracy.

ACKNOWLEDGMENT

The author would like to express their great appreciation to Geotech Ltd. The official distributor of Trimble navigation in Greece for the concession of the V10 imagine rover for the completion of the applications. We would also like to thank

Mr. Solonas Kitsinelis surveying engineer sales manager of Geotech Ltd. for his assistance, his felicitous remarks and his willingness to give his time so generously.

REFERENCES

- [1] Leica, "Leica Viva Smartstation", http://www.leica-geosystems.com/en/Leica-Viva-SmartStation_86610.htm, Last accessed November 13, 2015.
- [2] E. Lambrou, "Remote Survey: Alternative Method for Capturing Data". Journal of Surveying Engineering, 2013,
- [3] M. Scherer, and J. L. Lerma "From the Conventional Total Station to the Prospective Image Assisted Photogrammetric Scanning Total Station": Comprehensive Review. Journal of Surveying Engineering, Vol. 135, No. 4, November 2009.
- [4] G. Pantazis, E. Lambrou, S. Polydoros, and V. Gotsis, "3D Digital Terrestrial Model Creation Using Image Assisted Total Station and Rapid Prototyping Technology". International Journal of Heritage in the Digital Era. 10.1260/2047-4970.2.2.245, 245-262. Online publication date: 1-Jun-2013, 2013.
- [5] K. Kraus, "Photogrammetry". Dümmler, Bonn. Vol.1: Fundamentals and Standard Processes. Vol.2: Advanced Methods and Applications. Available in German, English & several other languages, 1997
- [6] C. Ellum, N. El-Sheimy, "Land-based mobile mapping systems". Photogrammetric Engineering and Remote Sensing, 68 (I), 13-17 (and 28), 2002.
- [7] J.K. Park, D.Y. Um "Accuracy Analysis of Structure Modeling using Continuous Panoramic Image", International Journal of Smart Home, Vol. 9, No. 5, May 2015, pp. 165-174, (<http://dx.doi.org/10.14257/ijsh.2015.9.5.16>), 2015.
- [8] A. Brunn, Th. Meyer, "Calibration of a Multi-Camera Rover", The International Archives of the Photogrammetry, Remote Sensing and Spatial Information Sciences, 2016, Volume XLI-B5, 2016 XXIII ISPRS Congress, 12-19 July 2016, Prague, Czech Republic.
- [9] A.G. Kampouris, "Assessment of the Three-Dimensional Integrated Camera System V10 Imaging Rover", Diploma Thesis (in Greek), School of Rural & Surveying Engineering, NTUA, Athens, 2015.
- [10] Trimble Navigation Limited 2008. Sunnyvale, California 94085, 2009. "User's manual for Trimble VX"
- [11] Trimble, 2015, "Trimble V10 Imaging Rover Datasheet", 2015, (www.trimble.com)
- [12] Trimble, "Trimble V10 Imaging Rover User Guide", revision A, Part Number 57047029, 2014, (www.trimble.com)
- [13] ISO/TR 7507-6, "Petroleum and liquid petroleum products - Calibration of vertical cylindrical tanks - Part 6: Recommendations for monitoring, checking and verification of tank calibration and capacity table", 1997
- [14] ISO 7507-1, "Petroleum and liquid petroleum products - Calibration of vertical cylindrical tanks - Part 1: Strapping method", 2003
- [15] API Standard 653, "Tank Inspection, Repair, Alteration, and Reconstruction", 5 ed., 2014



ISSN: 2277-3754

ISO 9001:2008 Certified

International Journal of Engineering and Innovative Technology (IJET)

Volume 6, Issue 6, December 2016

- [16] Paul R. Wolf and Charles D. Ghilani, "Adjustment Computations: statistics and least squares in surveying and GIS", John Wiley and Sons, Inc, New York. ISBN 0-471-16833-5, 1997.
- [17] A.M. Agatza-Balodimou, "Error Theory & Adjustments", Vol. I & II, Undergraduate Notes (in Greek) School of Rural & Surveying Engineering, NTUA, 2009.